Pressure Cell Assisted Solubilization of Xyloglucans: Tamarind Seed Polysaccharide and Detarium Gum

David R. Picout,*,† Simon B. Ross-Murphy,† Neil Errington,‡ and Stephen E. Harding‡

Biopolymers Group, Division of Life Sciences, King's College London, Franklin-Wilkins Building, 150 Stamford Street, Waterloo, London SE1 9NN, U.K., and National Centre for Macromolecular Hydrodynamics, School of Biosciences, University of Nottingham, Sutton Bonington, Loughborough LE12 5RD, U.K.

Received December 17, 2002; Revised Manuscript Received March 14, 2003

To improve the solubilization of two water-soluble xyloglucans, tamarind seed polysaccharide and detarium gum, by reducing substantially molecular aggregation, a "pressure cell" heating method was used. Conditions allowing solubilization and chain depolymerization were produced by varying appropriately the pressure, time, and temperature applied. The various MW fractions of solubilized xyloglucans were characterized by capillary viscometry and light scattering techniques in order to extract, with reliability, fundamental macromolecular parameters. Mark−Houwink and Flory exponents were found to be 0.67 ± 0.04 and 0.51 ± 0.06, respectively for both xyloglucan data combined, consistent with linear random coil behavior. A detailed analysis of the data seems to suggest that tamarind gum solutions are slightly perturbed by the effect of excluded volume, whereas detarium gum samples are close to the θ state. Chain flexibility parameters such characteristic ratio, C_∞, and persistence length, L_p, were calculated for tamarind and detarium using the Burchard-Stockmayer-Fixman (BSF) geometric method. L_p values of 6−8 nm were estimated for xyloglucans. The seemingly linear structure of tamarind and detarium, as suggested by the value of the Mark−Houwink and Flory exponents obtained, follows from analysis of the data by the classical Zimm method but not when employing the square root or Berry method which suggests a more branched chain profile. This was the approach adopted in our previous work on the characterization of detarium samples.

Introduction

Xyloglucans are a major class of structural polysaccharides found in the primary cell walls of higher plants. Cell growth and enlargement are controlled by the looseness of a thin net of microfibrils made of cellulose. Xyloglucan cross-links these cellulose microfibrils and provides the flexibility necessary for the microfibrils to slide.[1,2] Xyloglucan polysaccharide has the same skeleton, β-1,4 D-glucan, as cellulose and therefore is not digested by human digestive enzymes (it acts as dietary fiber). The cellulose backbone of xyloglucan is partially substituted by α-(1 6)-linked xylose units. Some of the xylose residues are β-D-galactosylated at O-2. It is known that the distribution of side chain residues is different in the xyloglucans from different species and it has even been shown to differ slightly, but significantly, between two natural populations of the same species growing in different environments.[3]

Tamarind seed polysaccharide is the major polysaccharide constituent of seeds from the tree *Tamarindus indica*. The seeds contain xyloglucans and are used extensively as food thickeners, stabilizers and gelling agents in Japan. In the USA, its major industrial use has been as a wet end additive in the paper industry as a replacement for starches and galactomannans.

Table 1. Results of Dionex HPAE Chromatography Showing Quantitatively Oligosaccharide Fractions Converted from Detarium and Tamarind Xyloglucan when Treated with *endo*-1,4-β-Glucanase [From Wang et al. (1996)][5]

	Oligosaccharide ratio[a]				Deduced monosaccharides		
	XXXG	XLXG	XXLG	XLLG	xylose	galactose	glucose
tamarind	1.00	0.42	2.07	6.20	1.00	0.51	1.34
detarium	1.00	0.30	5.60	6.20	1.00	0.46	1.33

[a] Standard nomenclature used.[31−33]

Detarium senegalense Gmelin, the seed flour of an African leguminous plant traditionally used in Nigeria for its food thickening properties in soups and stews, was also found to contain a high proportion of xyloglucans. Its structural composition is very similar to tamarind xyloglucan,[4] the main difference in terms of simple composition being in the proportion of galactose, relative to xylose and glucose. Table 1 from Wang and co-workers[5] shows the structural differences between these two xyloglucans.

Like many other polysaccharides, tamarind xyloglucan and detarium xyloglucan are water-soluble, but their individual macromolecules tend not to fully hydrate and consequently supramolecular aggregated species remain present even in very dilute solutions. This is because the $\beta(1 \rightarrow 4)$, cellulose-like backbone promotes interchain interactions, and so the polymers show a balance between hydrophobic and hydrophilic character. Light scattering techniques employed to

* To whom correspondence should be addressed. Phone: +44 (0) 20 7848 4246. Fax: +44(0) 20 7848 4082. E-mail: david.picout@kcl.ac.uk.
† King's College London.
‡ University of Nottingham.

10.1021/bm0257659 CCC: $25.00
Published on Web 04/11/2003

characterize such polymers in solution have not been very successful in providing good reliable data because of the nonhomogeneity of these solutions at the molecular level. Certainly, poor reproducibility may be the reason few light scattering results have been published so far. The architecture of tamarind seed xyloglucan, for example, has been investigated by light scattering, small-angle X-ray scattering (SAXS) and synchrotron radiation.[6] The data appeared to show that tamarind in aqueous solution consisted of multistranded aggregates, with a high degree of particle stiffness but no reproducibility of the molar mass was achieved. Various M_ws values for tamarind, 115 000[7] or 650 000[8] (GPC) or 880 000[9] (light scattering) or even 2 500 000[6] were reported in the literature. In this work as in our earlier contributions, we define M_w as relative weight average molecular mass, without units.

These variations are due to a strong tendency to self-association of the polysaccharide, and it is possible that these studies may have been affected by using non "molecular" solutions in which the materials were not fully solubilized. The problem of the characterization of the solution properties of water soluble polymers is long-standing, and in order to circumvent such problem, the pressure cell solubilization method originally employed by Vorwerg and co-workers on solutions of starch[10,11] has been proven to be appropriate and effective. This pressure/temperature solubilization approach subsequently applied with success to nonstarch polysaccharides such as detarium gum[12] and a series of galactomannans[13,14] is now employed in the present work to obtain "molecular" solutions of tamarind seed polysaccharide. Detarium xyloglucan will be recharacterized in this work but using a more complete range of pressure cell treatments and in order to be compared directly with tamarind using the same experimental conditions and characterization techniques. By achieving full solubilization and by reducing, substantially, time-dependent aggregation phenomena in this study, we are able to characterize the two polymers mentioned above. In this way, we hope to obtain reliable light scattering data, which tend to be scarce for such xyloglucans. Using appropriate models, we intend to calculate various parameters such as the Mark−Houwink and Flory exponents, the characteristic ratio, and the persistence length of both polysaccharides in order to obtain molecular information such as chain flexibility and shape.

Experimental Section

Materials. Purified samples from commercial grade tamarind xyloglucan polysaccharide (cold water soluble) were supplied by Dainippon Pharmaceutical Co. Ltd., Tokyo, Japan. The samples were purified from the flour using an isolation procedure devised by Girhammar and Nair,[15] and modified by Rayment et al.[16] to allow complete hydration of the gum. The moisture content of the extracted polymer was determined by incubation overnight in an oven at 103 °C to a constant weight. Freeze-drying was carried out using an Ehrist ALPHA I-5 Freeze-dryer (DAMON/IEC (U.K.) Ltd.), and samples were stored in a desiccator until used. The detarium xyloglucan used in this study has been purified in the same way as for tamarind; the extraction procedure of the detarium flour from the seed samples purchased at a local market in Nsukka, Enugu State, Nigeria is described in ref 5.

Table 2. Summary of Intrinsic Viscosity [η] and Static Light Scattering Results (Using the ALV System) for Tamarind Seed Polysaccharide.

sample	treatment	[η] (dL/g)	M_w ($\times 10^{-6}$) [a]	R_g [b] (nm)	A_2 ($\times 10^4$) [c]
tamarind	untreated	6.15	IR	IR	IR
	100 °C, 30 min, 4 bar	6.1	0.83	136	21
			0.79	133	18
	130 °C, 10 min, 4 bar	5.9	0.77	114	11
			0.75	115	12
	130 °C, 10 min	6.05	0.73	103	6
			0.71	99	7
	130 °C, 20 min	5.85	0.67	101	6
			0.68	100	7
	130 °C, 30 min	5.65	0.64	94	12
			0.65	100	7
	130 °C, 60 min, 4 bar	5.45	0.56	94	10
			0.54	97	10
	130 °C, 60 min	5.35	0.56	92	9
			0.58	95	10
	160 °C, 10 min, 4 bar	4.7	0.52	93	10
			0.56	98	12
	160 °C, 10 min	4.35	0.50	83	11
			0.52	93	6
	160 °C, 30 min	4.0	0.49	89	14
			0.45	89	11

[a] Mw corresponds to the zero concentration and zero angle extrapolations of the Zimm plot. [b] $R_g = z$ average root-mean-square radius of gyration. [c] A_2 = second virial coefficient in units of reciprocal concentration, viz. mol mL/g^2. IR = irreproducible results.

Methods. Dilute solutions of tamarind and detarium gum were prepared at 0.05 wt %, i.e., below C* defined as 1/[η], by adding known weights of the freeze-dried samples to deionized water at 50 °C, containing 0.02% sodium azide as bactericide. The temperature was raised to 80 °C as dry powder was added with stirring. The heating was stopped as soon as 80 °C was reached and the solutions were left covered overnight, with stirring, at room temperature to allow further hydration to occur.[17] The solution at this stage was used as a reference material ("untreated sample"). A total of 30 mL of this solution was then added to the reaction chamber of a pressure/heating cell (HEL Ltd, Barnet, Herts. U.K.). These solutions were then subjected, under stirring, to a range of temperature and pressure conditions between 70 and 160 °C and 0−4 bar added pressure. Added pressure was applied using nitrogen gas while the reaction chamber was at a temperature of 50 °C. These conditions were applied for a range of times from 10 to 60 min. The general protocol is described in more detail in ref 12.

The treated solutions were then analyzed using several techniques:

1. Capillary Viscometry. The intrinsic viscosities [η] given in Tables 2 and 4 were determined using the Viscosity Measuring Unit AVS 350 (Schott-Geräte, Hofheim, Ger-

Table 3. Summary of Intrinsic Viscosity [η] and Static Light Scattering Results (SEC/MALLS) for Tamarind Seed Polysaccharide.

sample	treatment	[η] (dL/g)	M_w ($\times 10^{-6}$)	R_g (nm)
tamarind	70 °C, 10 min	6.7	0.80	115
			0.73	97
	100 °C, 10 min	6.5	0.76	106
	100 °C, 10 min, 4 bar	6.15	0.74	101
	130 °C, 10 min	6.0	0.64	101
	130 °C, 10 min, 4 bar	5.4	0.64	101
			0.68	104
	130 °C, 30 min, 4 bar	5.15	0.61	104
			0.56	92

Table 4. Summary of Intrinsic Viscosity [η] and Static Light Scattering Results (Using the ALV System) for Detarium Gum.

sample	treatment	[η] (dL/g)	M_w ($\times 10^{-6}$)[a]	R_g[b] (nm)	A_2 ($\times 10^4$)[c]
detarium	untreated	8.7	IR	IR	IR
	100 °C, 10 min, 4 bar	8.8	1.66	119	3
			1.63	114	3
	130 °C, 10 min, 4 bar	8.3	1.25	120	3
			1.20	110	5
	130 °C, 10 min	8.0	1.25	103	-1
			1.27	107	-1
	130 °C, 20 min	7.8	1.15	109	-1
			1.10	110	-2
	130 °C, 30 min	7.25	1.08	130	-1
			1.07	127	-1
	130 °C, 60 min, 4 bar	7.35	1.07	123	-1
			1.11	126	2
	160 °C, 10 min, 10 bar	6.5	0.8	102	-5
			0.82	99	-5
	160 °C, 10 min	5.5	0.75	84	-6
			0.67	80	-8
	160 °C, 30 min	4.9	0.63	73	-5
			0.64	75	-5

[a] M_w corresponds to the zero concentration and zero angle extrapolations of the Zimm plot. [b] $R_g = z$ average root-mean-square radius of gyration. [c] A_2 = second virial coefficient in units of reciprocal concentration, viz. mol mL/g^2. IR = irreproducible results.

many), connected to a ViscoDoser AVS 20 Piston Buret (for automatic dilutions). This makes automated measurements of the flow-through times in a capillary viscometer (Ubbelhode viscometer for dilution sequences). The viscometer was immersed in a precision water bath (transparent thermostat CT 1650, Schott-Geräte, Hofheim, Germany) to maintain the temperature at 25 ± 0.05 °C. All polymer concentrations ranged from 0.01 to 0.05% (w/v) so that the viscosity relative to that of the solvent (water) lay in the range $1.2 < \eta_r < 2.0$. Results were analyzed using separate Huggins and Kramer extrapolations (linear regression, 99% confidence intervals) and the final result quoted in dL/g (1 dL/g = 100 mL/g = 0.1 m^3/kg).

The intrinsic viscosities [η] in Table 3 were determined using an alternative Viscosity Measuring Unit (AVS 400, Schott-Geräte, Germany) and a capillary viscometer (Ubbelohde type for dilution series) to make automatic measurements of solution and solvent flow times. The viscometer was immersed in a precision water bath at (25.00 ± 0.05)°C (CT1450 water bath with DLK400 refrigeration unit, Schott-Geräte, Germany) and 10 replicate measurements made on each solution. Results were analyzed as described above.

2. Size Exclusion Chromatography Coupled to Multiangle Laser Light Scattering (SEC/MALLS). The size exclusion chromatography system used consisted of Jasco HPLC pump, a guard column and TSK G5000 and G4000 columns. An on-line degasser was used to remove gas from the eluent. A flow rate of 0.8 mL/min for the mobile phase was used at room temperature. A DAWN-DSP multiangle laser light scattering detector and an Optilab 903 refractometer (Wyatt Technologies, Santa Barbara, CA) were used for light scattering intensity and concentration detection, respectively. The mobile phase was 0.02-weight % sodium azide in distilled de-ionized water. 100 μL samples of the tamarind solutions were injected into the size exclusion system after filtering through 0.45 μm filters (Whatman Ltd., Maidstone, England). Repeat injections were made for each sample. Data were captured and analyzed using the software package ASTRA (v. 4.20). Data returned are the number, weight, and *z* averages for molecular weight and root-mean-square radius of gyration. These measurements were performed only for some of the tamarind samples (Table 3).

3. Static and Dynamic Light Scattering. These measurements were performed simultaneously, i.e., both in static and dynamic mode, on the same photons, at 20 °C with a fully computerized ALV-5000 System comprising a compact goniometer system and a multi-τ real-time digital correlator (ALV−Laser Vertriebsgesellschaft m.b.H, Langen, Germany). The angular range applied was from 30° to 150° in steps of 10°; the duration of single measurements was typically 10 s averaged over a minimum number of 3 runs until a statistically significant result was obtained in static mode (ALV/Static & Dynamic Fit and Plot Program used). Although dynamic data were calculated our approach was to concentrate on the quality of the static data. A He−Ne laser ($\lambda_0 = 632.8$ nm) was the light source, and the scattering of toluene was used as the primary standard. The refractive index increment, d*n*/d*c*, was chosen as 0.146 mL g^{-1}. [18] Solutions used for light scattering were solutions of 0.05% polymer (prepared as described previously and treated in the pressure cell appropriately) and serial dilutions (0.04%, 0.03%, 0.02%, and 0.01%). These solutions were filtered 3 times directly into the cylindrical light scattering cuvettes (Pyrex disposable culture tubes, Corning Incorporated, Corning, New York) (total volume ~3 mL) using Acrodisc PF 0.8/0.2 μm syringe filters (Gelman Laboratory, Michigan). All solution preparation stages were carried out in a laminar airflow cabinet to minimize contamination with dust. Here both tamarind and detarium gum samples were used.

Results and Discussion

[η] Determination. The intrinsic viscosities [η] of the tamarind samples after various pressure cell treatments (or none) are shown in Tables 2 and 3. Table 4 displays the intrinsic viscosities obtained for detarium gum after being

subjected to similar treatments under combined temperature, time, and pressure regimes. The data clearly show that the intrinsic viscosity variation for both xyloglucans is minimal with increasing temperature up to around 130 °C (with or without excess pressure) unless the time of treatment is increased considerably (>10 min). When temperature is increased to 160 °C, [η] values decrease more sharply. This phenomenon is not surprising and has been previously reported for a series of galactomannans in our two previous papers;[13,14] the observed effect is consistent with thermal degradation of the polymers chains. When excess pressure is applied (4−10 bar), in most cases, [η] is higher than for the samples treated at the same temperature and time conditions but without the excess pressure. This is observed especially at the highest temperatures used (160 °C), whereas at lower temperatures, [η] does not vary much as mentioned before. The addition of excess pressure in the treatment of xyloglucans seems to "protect" the polysaccharide chains from some of the degradation effect, as also observed for galactomannans.[13,14] Speculations have been made on the effect of pressure on chain degradation,[13] but the reasons still remain unclear.

***M*$_w$ and *R*$_g$ Determination.** Light scattering techniques were used in order to collect M_w (weight-average molecular weight) and R_g (z average root-mean-square radius of gyration or more formally $\langle S^2 \rangle_Z^{1/2}$) data on all of the samples. Our facilities enabled us to use two types of light scattering instruments. As mentioned above, the ALV-5000 system was used to characterize the detarium samples and some of the tamarind samples. From the light scattering static mode M_w, R_g, and A_2 (the second virial coefficient) were obtained from the appropriate Zimm plots by extrapolation of the experimental data to $c = 0$ and $q^2 = 0$ using fitted polynomials (Table 2 and Table 4). SEC/MALLS was used only for the M_w and R_g determination of a few treated tamarind solutions (Table 3). Light scattering measurements were also made on six untreated samples of tamarind and three untreated samples of detarium. Particle molar mass values obtained ranged from 0.48×10^6 to 1.14×10^6 for tamarind and from 1.5×10^6 to 2.4×10^6 for detarium gum, showing the difficulty in obtaining reproducible data and, therefore, their reliability. R_g values obtained were also very different from each other leading us to the observation that untreated samples are practically impossible to characterize by light scattering because of the strong presence of aggregates.

Indeed, aggregates can cause distortions in the angular dependence of scattered light and thus lead to errors in the determination in the intercept on the scattering intensity (K_c/R_θ) axis, leading to a false and nonreproducible estimation of M_w and R_g. As can be seen in the various tables (2−4), pressure cell treated samples, however, give good and reproducible light scattering results. Solubilization has improved with the pressure cell heating method, suggesting that the aggregates have been reduced or even been fully hydrated.

Mark−Houwink-Sakurada (MHS) and Flory Exponents. Figure 1 shows the MHS plot (log [η] vs log M_w) constructed using all of the experimental data on the samples of tamarind and detarium combined. The MHS exponents α

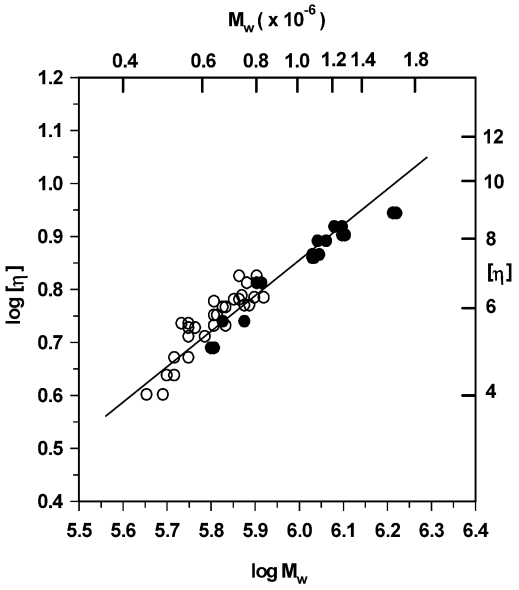

Figure 1. Mark−Houwink−Sakurada plot (log[η] vs log M_w) for tamarind (○) and detarium (●) samples treated under various temperature, time, and pressure conditions. The slope (the exponent) is 0.67 ± 0.04.

obtained from the slope for the double logarithmic plot of intrinsic viscosity against M_w are 0.76 ± 0.07 and 0.62 ± 0.04 for tamarind and detarium, respectively. These values are approximately within the bounds of the Mark−Houwink equation for linear flexible macromolecules.

To get a value of the MHS exponent for both xyloglucans combined, a statistical analysis of covariance was carried out on the two sets of data using Minitab statistical software release 13.1 (Minitab Inc., Pennsylvania). It was found that there were no significant differences in slopes between the two sets of data, but a significant difference in the two intercepts (the usual goodness of fit, $P < 0.0005$) was found. To obtain the best slope representative of all of the data, a set of two parallel lines was fitted to the data. The slope calculated was found to be 0.67 ± 0.04 for both xyloglucans combined, giving an MHS exponent α well within the known limits 0.5−0.8 found in the literature for a polymer chain in the so-called flexible coil conformation. This linear conformation is further supported by Figure 2, which represents the double log plot of R_g against M_w for the tamarind and detarium data. The Flory exponents obtained for tamarind and detarium separately are 0.54 ± 0.07 and 0.49 ± 0.09, respectively, and lie close to or within the expected range 0.5−0.6. The lines shown in Figures 1−2 are for guidance only. They are representative of the best slope for all the data and do not represent the best fit as in fact not one line but a set of parallel lines was fitted into the data.

The statistical analysis of covariance of the two sets of data (no significant differences between the two slopes but differences between the intercepts) enabled the calculation of the best-fitted slope for tamarind and detarium data together. The Flory exponent was found to be 0.51 ± 0.06, being close to the Flory-theta chain, 0.5, value which seems to suggest that xyloglucans have a linear coil conformation but without excluded volume. As we discuss later, there is an inconsistency between α, and this exponent in terms of the excluded or no excluded volume concept.

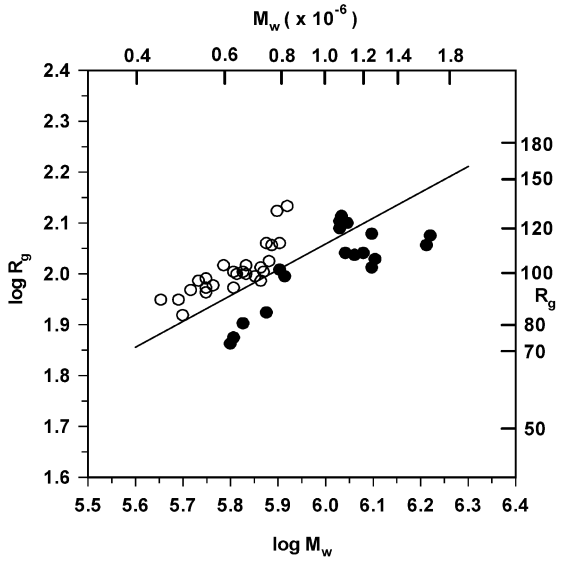

Figure 2. Values of radius of gyration, here R_g plotted as a function of (weight average) M_w for the tamarind (○) and detarium (●) data. The Flory exponent is 0.51 ± 0.06.

Structural Architecture of Xyloglucans. In the literature, there is no strong evidence about the structural architecture of xyloglucans, and it is not clear whether xyloglucan macromolecules are linear or long chain branched. Detarium xyloglucan solutions were studied by Wang and co-workers,[5] and they found that semidilute solution characterization work was very consistent with much of the published data for the rheology of other polysaccharide solutions. The data suggested that detarium gum was a well-behaved linear polymer entanglement network system. However, light scattering measurements carried out by the same group on dilute solutions of detarium showed that the scattering profile was not consistent with that of a linear macromolecule, but instead strongly suggested a small degree of long chain branching.

By contrast, the MHS and Flory exponents calculated in our study tend to suggest that tamarind and detarium macromolecules are linear. Because the quality of the zero concentration data obtained from the Zimm plots for both xyloglucans is highly acceptable, we adopt a well-known procedure to examine the shape of the macromolecules using the so-called Kratky plot.[19] It is important to note that this procedure is widely employed for both synthetic and biopolymers using small-angle X-ray light scattering (or, even light scattering for high molecular weight polymers) but that it is not such an ideal approach to use for light scattering of polysaccharides or other water soluble polymers. This is because the overall data are usually not reliable for the angular region above 60° or at most 90° because of a lack of scattering and because the M_ws of the macromolecules are generally not high enough (W. Burchard, personal communication). However, this approach has been successful[20] with very high M_w polysaccharides ($> 2 \times 10^7$) such as branched amylopectin and glycogen or with very stiff macromolecules such as xanthan.

Parts a and b of Figure 3 show a Kratky plot for four tamarind and four detarium samples, respectively, treated under various temperature, time, and pressure conditions. Here $u = qR_g$, $P(u) \equiv R_\theta/R_{\theta=0}$ is the so-called particle

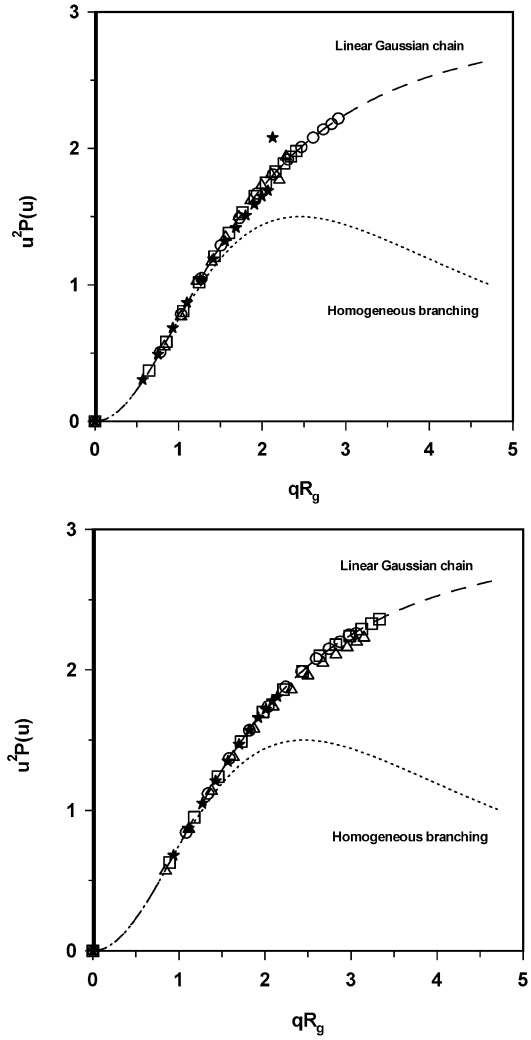

Figure 3. (a) Kratky plot constructed using conventional Zimm plot data for tamarind samples treated under various conditions: (○) 130 °C, 10 min, 4 bar; (□) 130 °C, 30 min; (△) 130 °C, 60 min; (★) 160 °C, 10 min. Theoretical curves calculated for models as in Burchard.[20] The dashed line represents linear Gaussian chains and the dotted line is for homogeneous branching. (b) As Figure 3a for detarium samples: (○) 130 °C, 10 min, 4 bar; (□) 130 °C, 30 min; (△) 130 °C, 60 min, 4 bar; (★) 160 °C, 10 min.

scattering factor, which reflects the angular dependence of the scattered light, and q is the magnitude of the scattering vector ($=4\pi\lambda/\sin(\theta/2)$). The dimensionless parameter u, measures the intramolecular probe distance relative to the incident light wavelength, and $P(u)$ can be calculated for different chain architectures. The two different curves represented in Figure 3, parts a and b, reflect fits to different models for the chain behavior, the upper dashed line representing the theoretical profile for a flexible Gaussian chain and the lower dotted line illustrates the corresponding profile for a high degree of random homogeneous branching.[19] Experimental data are shown with different symbols. R_g values were obtained from light scattering measurements using the Zimm plot. From the plots, it can be seen that the experimental data, both for tamarind and detarium, follow the linear chain model rather well. However, if good Zimm plot data are reanalyzed in terms of the Berry plot, and then zero angle data replotted in terms of $u^2P(u)$ versus u, the same experimental data plotted in Figure 3, parts a and b,

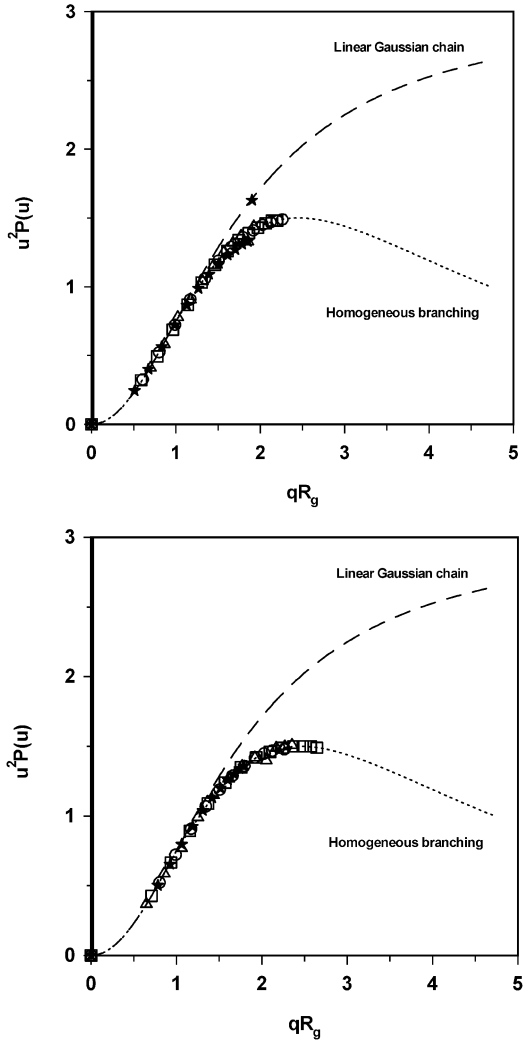

Figure 4. (a) As Figure 3a, but with the Kratky plot constructed using Berry plot analysis for tamarind samples: (○) 130 °C, 10 min, 4 bar; (□) 130 °C, 30 min; (△) 130 °C, 60 min; (★) 160 °C, 10 min. Again the dashed line and the dotted line represent linear Gaussian chains and homogeneous branching models, respectively. (b) As Figure 4a for detarium samples: (○) 130 °C, 10 min, 4 bar; (□) 130 °C, 30 min; (△) 130 °C, 60 min, 4 bar; (★) 160 °C, 10 min.

now appear to follow the homogeneous branching model more closely, as shown in Figure 4, parts a and b.

Zimm and Berry Plot Analysis. The classical approach[21] to processing light scattering data is to produce the so-called Zimm plot of K_c/R_θ versus a linear function of $\sin^2(\theta/2)$ (angular dependence) and c (concentration dependence). The linear function is chosen in such a way that the three-dimensional surface of $\sin^2(\theta/2)$ and c is compressed into a plane. This approach is still widely employed, but for very high molecular weight, or less flexible polymers, the angular dependent "upswing" means the usual simultaneous linear extrapolation to $\sin^2(\theta/2)\rightarrow 0$ and $c \rightarrow 0$ to give $K_{c=0}/R_{\theta=0} = (1/M_w)$ is distorted. An alternative approach by Berry[22] plots $(K_c/R_\theta)^{1/2}$ vs $\sin^2(\theta/2)$ and c. This does linearize the upturn effect described above, but this is an explicit weighing of the data. The ALV system can extrapolate data either in Zimm or Berry coordinates, but results obtained, particularly for $c \rightarrow 0$ are, of course, not the same. This actually distorts the apparent angular dependence of $K_{c=0}/R_\theta$, in a way which appears to alter the profile very significantly as we can see

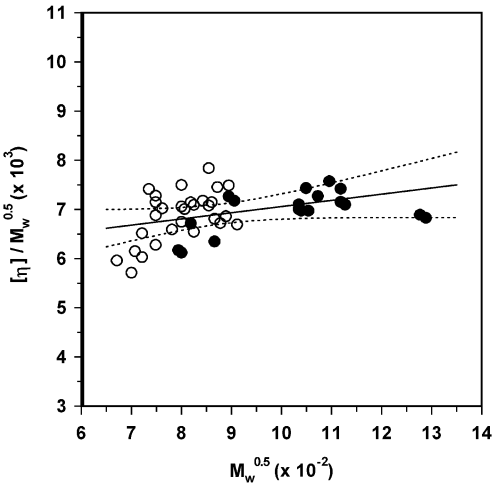

Figure 5. BSF plot ($[\eta]/M_w^{1/2}$ vs $M_w^{1/2}$) for tamarind (○) and detarium (●) data. Dotted lines indicate 99% confidence intervals.

from Figures 3 and 4. It seems therefore that depending upon the method used for the determination of M_w and R_g (Zimm or Berry plots) very different final conclusions can be drawn. We wish to point out here that although the angular distribution is linear in the Zimm plot, we also applied the Berry plot method simply for comparison with the data obtained in our initial paper on detarium.[12] In this paper, we deduced the presence of branching from the Berry plot. However, comparison of the results from this paper with the present set seems to suggest that the earlier samples had too low an $[\eta]$ value for the measured Mw. The branching may therefore be actually due to insufficient deaggregation, whereas the same is not seen here. To clarify whether branching or insufficient deaggregation is achieved we would probably need small-angle X-ray rather than light scattering.

The reasons for these differences in the two methods are unclear, but in any case, it can be said that if only the data in the angular region below 60° were to be reliable, in the Kratky approach, then all data would almost lie in the overlapping region of the two theoretical models. Therefore, no strong conclusions can be drawn on the shape of these xyloglucan macromolecules from the Kratky approach. This follows because the wavelength of the HeNe laser used in the present work is too high ($\lambda_0 = 632.8$ nm) for the size of the macromolecules measured (~80 nm for R_g) and hence there is almost no shape information.

Chain Flexibility of Xyloglucans. To determine the chain characteristic ratio, C_∞, and the persistence length, L_p, of flexible to semiflexible polymers, one common plot used is that due to Burchard et al. (BSF plot)[23] in which $[\eta]/(M_w)^{1/2}$ is plotted against $(M_w)^{1/2}$. The BSF method was applied to the tamarind and detarium data separately and to the combined data. Figure 5 shows the BSF plot for all tamarind and detarium data combined. Statistical analysis was carried out on the two sets of xyloglucan data. Both sets showed significant differences between the slopes and between the intercepts, but this was only due to a few tamarind data (samples treated at 160 °C), which were in our opinion increasing the slope artificially. Because we have less confidence in these data sets, we consider that the best way of analyzing the overall data is in fact to regard them as one

Table 5. Determination of MHS and Flory Exponents, Characteristic Ratios C_∞ and Chain Persistence Lengths L_p for Detarium and Tamarind Xyloglucans.

				Burchard−Stockmayer−Fixman (BSF) method	
samples	residue m_r[a]	MHS exponent	Flory exponent	C_∞	L_p (nm)
detarium	434	0.62 ± 0.04 (SE)	0.49 ± 0.09 (SE)	25 ± 4 (SE)	5−8
tamarind	445	0.76 ± 0.07 (SE)	0.54 ± 0.07 (SE)	19 ± 4 (SE)	4−6
both xyloglucans	∼440	0.67 ± 0.04 (SE)	0.51 ± 0.06 (SE)	26 ± 2 (SE)	6−8

[a] Calculated from the structure reported by Wang et al.[5] SE = standard error.

population. Using a simple regression analysis will obtain the best slope and intercept representing all of the data combined.

From the BSF plots, the intercept K_θ (which corresponds to the chain in the θ state, where there is no excluded volume) was obtained and from the MHS equation and the Flory Fox equation, C_∞ and then L_p were calculated for both polymers individually and also for all the data combined. Detailed methods are given, for example, in ref 13.

Table 5 summarizes the MHS and Flory exponents, characteristic ratio, and chain persistence lengths calculated for tamarind and detarium xyloglucans. The molar masses of the polymer residues used in the calculation of the characteristic ratios, C_∞, were calculated for tamarind and detarium using the deduced monosaccharides ratio attributed to these two polymers (see Table 1) and are shown in Table 5. For all xyloglucan data combined, the persistence length, L_p, calculated was found to be 6−8 nm. This is reasonably close to, if slightly larger than, the L_p values found in the literature for cellulose and derivatives,[24] which is not too surprising because xyloglucans have a cellulosic backbone. Compared to the L_p values obtained for galactomannans,[14,25] the xyloglucan L_p values calculated here are slightly higher suggesting that xyloglucan chains are stiffer (in relative terms) than galactomannan chains but may still be considered relatively flexible compared to very stiff macromolecules such as xanthan ($L_p \sim 120$ nm[26]).

Validity of Methods Employed. In this study as in our earlier papers, we have employed the Burchard−Stockmayer−Fixman method to extrapolate to lower chain length, to estimate such parameters as the persistence length L_p and the chain characteristic ratio C_∞. There is no doubt this approach could be criticized on a number of grounds. First, the method itself is only one (albeit the simplest) of several methods and has, in the past, been censured on a number of grounds. For example, it is well-known[27] that, with decreasing chain length, chain hydrodynamic effects, the so-called draining term in the Flory−Fox equation, change, and for rods and semiflexible chains, the effect can be marked. The effect of increased draining causes a decrease in Flory's viscosity constant Φ or draining parameter, which can, in turn produce a distortion in the BFS plot. We also comment that direct measurements of L_p, for example from small-angle X-ray scattering measurements, are often somewhat larger than the BSF extrapolated values, but currently, such measurements have to be made at substantially greater concentrations. Nevertheless, the lower chain stiffness found from BFS plots has been known historically. That said, the difference is usually not so great, typically ∼30%, which is about the absolute error of the present measurements.

More seriously, perhaps, is the argument whether these chains are indeed perturbed by excluded volume or whether all of the effects seen are due to intrinsic chain stiffness? In practice, it is extremely difficult to separate these two effects for systems when the persistence length itself is comparatively low (say <∼10 nm). By contrast for the ultra-stiff polymers xanthan and schizophyllan polymers ($L_p \sim 120$ and 180 nm, respectively[26,28,29]), it is reasonable to assume there is almost no excluded volume. For these polymers, the chains adopt a helical structure, this in turn results in the high L_p. Here the number of persistence lengths in the chain contour length L is typically small. We observe it is more usual to revert to Kuhn lengths, L_k, where $L_k = 2L_p$, and then define the number of Kuhn segments n_k as L/L_k. For xanthan and schizophyllan systems, n_k is typically ∼2−6, so by the usual criteria, i.e., $n_k \geq 6-10$, these are not Gaussian chains.

If we consider an ideal polymer chain with n segments each of a length l, the contour length L is defined by $L = nl = n_k L_k$. The number of segments n represents the number of repeat units in the polymer chain and can be defined as $n = M_w/m$, where M_w is the weight-average molecular weight of the polymer and m is the relative molar mass of a residue (repeat unit). From all of the equations above, n_k can be rewritten as $n_k = M_w l/2mL_p$. When calculated for the tamarind and detarium samples using[23] $l = 0.54$ nm (the O−O virtual bond length for a 1,4-diequatorially linked residue), we found $55 < n_k < 100$ for tamarind and $60 < n_k < 160$ for detarium.

In the present case, for both tamarind and detarium, we have a more than sufficient value of n_k (n_k far greater than 6−10) to consider the chains as coil polymers, so we have to use other criteria to examine the contribution or, otherwise, of excluded volume effects. One of these is to consider the values of either the Mark−Houwink exponent α, or the Flory exponent of R_g and M_w. For the first exponent, we have values of ∼0.76 for tamarind and ∼0.62 for detarium. Both are significantly >0.5, the Flory or θ-state value, but less than the excluded volume asymptotic limit of 0.8. For the corresponding Flory exponent, we have values of 0.54 and 0.49, respectively (equivalent Flory limits 0.5 in the θ state and 0.6 in the excluded volume limit). This would suggest that tamarind gum solutions are indeed slightly perturbed by the effects of excluded volume, whereas detarium gum samples are close to the θ state. Qualitatively, at least, data for the second virial coefficient, A_2, support this assertion, corresponding values are typically $\sim 9 \times 10^{-4}$ mol mL/g^2 for tamarind, whereas the values for detarium are lower, and indeed some are slightly negative. However, all values are quite small, and the data are certainly not good enough, nor

is the range of M_w sufficiently wide, that we can investigate, for example, the M_w dependence of A_2. The BSF plot for detarium, Figure 5, can be approximated to a straight line parallel to the abscissa, even though that the data are scattered. For a clear θ system, with α and the Flory exponent both equal to 0.5, the plot is, of course, constrained to give a horizontal line.

For the tamarind data, there is clearly a finite slope, although the range of M_ws is even lower. This then poses a further question. Values of A_2 are quite low, which suggests there is little effect of excluded volume, but both α and Flory exponents tend to support the opposite conclusion. Could this simply be the effect of intrinsic chain stiffness alone? As we hinted above, there can be no clear answer to this without performing other experiments, perhaps using small-angle X-ray scattering, SAXS, classical hydrodynamics or from more detailed dynamic light scattering, giving access to Burchard's ρ parameter, the ratio of R_g to R_h, the Stokes radius. For this sample, dynamic light scattering (DLS) results were so scattered that we could come to no definitive conclusions on ρ. However, all of the R_h values (calculated from the Stokes−Einstein relationship) were significantly lower than the R_g values, but not lower than $\sim R_g/2$. This, at least, reduces the possibility of either rigid rod or homogeneous sphere architecture for xyloglucans. Future work ought to investigate the dynamic scattering behavior in more detail. However, such measurements can be extremely time-consuming.

This may, in fact, not be a real issue, as has been demonstrated in recent measurements by Norisuye and coworkers[30] for a semiflexible microbial polysaccharide system. Here, analysis with and without excluded volume produced estimates of $\sim 9 \pm 1$ and $\sim 11 \pm 1$ nm, respectively, suggesting that, in this range of stiffness (and, presumably, for lower values such as we estimate here), the overall difference is within experimental error.

Although some of the discussions here are, by their nature, speculative, it is interesting to consider what we can make of the values obtained. For detarium on its own, we have L_ps around 5−8 nm. This is slightly larger than for the galactomannans[13,14] (~4 nm). We also have some indication from Figure 5 that the value for tamarind is slightly lower than that for detarium. All this is, in fact, quite consistent with our earlier conclusions. For the relatively unsubstituted galactomannans, values reflect only the stiffness of the β-(1 → 4) backbone and, consequently, lie quite close to those for cellulose in nonaqueous solvents. We would then expect a slightly higher value for the more side-chain packed xyloglucans and with a slightly greater value for detarium than for tamarind. This reflects the greater proportion of the XXLG oligosaccharide fraction in detarium compared to tamarind [G = unsubstituted glucose residue; X = xylose substituted glucose residue; L = galactosylxylose substituted glucose residue; sequences always read toward the reducing end of the molecule[31−33]].[5] Because there is some evidence that xylose units are more hydrophobic than galactose and glucose units, our conclusions are consistent with expectation. Indeed, in xylose, the absence of the C(6) hydroxymethyl group causes a big reduction in conformational entropy; also because xylose has one less OH group than glucose and galactose, it can form fewer hydrogen bonds with water, being therefore more hydrophobic (E. R. Morris, personal communication). Besides, the main reason for a decrease in the entropy of mixing and in solubility is that the hydrophobic interaction causes a stronger clustering of the water in the neighborhood of the hydrophobic groups.

Conclusion

The method of solubilizing highly aggregated water-soluble polysaccharides using the pressure cell approach has been again applied successfully, this time with xyloglucan polysaccharides from tamarind and detarium legumes. The pressure-cell treated samples produced high quality reproducible light scattering data because of the absence of (or highly reduced) aggregates in solution. Fundamental macromolecular parameters relating to chain structure and chain flexibility were calculated. Mark−Houwink and Flory exponents with values of 0.67 ± 0.04 and 0.51 ± 0.06, respectively, were obtained for both xyloglucan data combined, and calculated L_ps of 6−8 nm suggest that tamarind and detarium behave as linear flexible (to semiflexible) coil polysaccharides, with the tamarind sample showing some perturbation from random coil behavior from excluded volume effects.

Interestingly, we failed to confirm the branched structure reported for detarium gum in earlier work.[12] Indeed evidence from this work suggests that such deductions are highly model dependent, because analysis of the data by the classical Zimm method suggested essentially linear chains, whereas employing the square root or Berry method, also commonly used in this area, suggests a more branched chain profile. We hope to have an opportunity to explore this apparent ambiguity in future. Despite this, the achievement of obtaining consistent and apparently reliable Mark−Houwink and Flory parameters for a second class of "difficult" polysaccharides was highly gratifying.

Acknowledgment. We thank the Biotechnology and Biological Sciences Research Council (BBSRC) for financing this project under Grant 29/D10446. We are also grateful to Dr. Peter Ellis, Division of Life Sciences, King's College London, for helpful discussions as well as Prof. E. R. Morris (Cork, Ireland), Dr. S. Radosta (Golm, Germany), Prof. T. Norisuye (Osaka, Japan), Prof. W. Burchard (Freiburg, Germany), and Prof. K. Kajiwara (Tokyo, Japan) for valuable comments.

References and Notes

(1) Hayashi, T. *Ann. Rev. Plant Physiology Plant Molecular Biol.* **1989**, *40*, 139.
(2) Whitney, S. E. C.; Brigham, J. E.; Darke, A. H.; Reid, J. S. G.; Gidley, M. J. *Plant J.* **1995**, *8*, 491.
(3) Reid, J. S. G.; Edwards, M. E. *Food polysaccharides and their applications*; Marcel Dekker: New York, 1995; p 155.
(4) Reid, J. S. G. *Adv. Botanical Res. Incorporating Adv. Plant Pathology* **1985**, *11*, 125.
(5) Wang, Q.; Ellis, P. R.; Ross-Murphy, S. B.; Reid, J. S. G. *Carbohydr. Res.* **1996**, *284*, 229.
(6) Lang, P.; Kajiwara, K. *J. Biomater. Sci.-Polym. Ed.* **1993**, *4*, 517.
(7) Glicksman, M. *Food hydrocolloids*; CRC Press: Boca Raton, FL, 1986; p 191.

(8) *Tamarind Seed Polysaccharide GLYCOID*; Dainippon Pharmaceutical Co., Ltd., 1989.
(9) Gidley, M. J.; Lillford, P. J.; Rowlands, D. W.; Lang, P.; Dentini, M.; Crescenzi, V. *Carbohydr. Res.* **1991**, *214*, 299.
(10) Aberle, T.; Burchard, W.; Vorwerg, W.; Radosta, S. *Starch-Starke* **1994**, *46*, 329.
(11) Vorwerg, W.; Radosta, S. *Macromol. Symp.* **1995**, *99*, 71.
(12) Wang, Q.; Ellis, P. R.; Ross-Murphy, S. B.; Burchard, W. *Carbohydr. Polym.* **1997**, *33*, 115.
(13) Picout, D. R.; Ross-Murphy, S. B.; Errington, N.; Harding, S. E. *Biomacromolecules* **2001**, *2*, 1301.
(14) Picout, D. R.; Ross-Murphy, S. B.; Jumel, K.; Harding, S. E. *Biomacromolecules* **2002**, *3*, 761.
(15) Girhammar, U.; Nair, B. M. *Food Hydrocoll.* **1992**, *6*, 285.
(16) Rayment, P.; Ross-Murphy, S. B.; Ellis, P. R. *Carbohydr. Polym.* **1995**, *28*, 121.
(17) Ellis, P. R.; Morris, E. R. *Diabetic Med.* **1991**, *8*, 378.
(18) Theisen, A.; Johann, C.; Deacon, M. P.; Harding, S. E. *Refractive increment data-book for polymer and biomolecular scientists*; Nottingham University Press: Nottingham, U.K., 2000.
(19) Burchard, W. *Adv. Polym. Sci.* **1983**, *48*, 1.
(20) Burchard, W. In *Physical Techniques for the Study of Food Biopolymers*; Ross-Murphy, S. B., Ed.; Blackie Academic and Professional: Glasgow, 1994; p 151.
(21) Zimm, B. H. *J. Chem. Phys.* **1948**, *16*, 1099.
(22) Berry, G. C. *J. Chem. Phys.* **1966**, *44*, 4550.
(23) Morris, E. R.; Ross-Murphy, S. B. *Tech. Carbohydr. Metab.* **1981**, *B310*, 1−46.
(24) Ross-Murphy, S. B. In *Cellulose Chemistry and its applications*; Nevell, T. P., Zeronian, S. H., Eds.; Ellis Horwood Ltd.: Chichester, U.K., 1985; p 202.
(25) Robinson, G.; Ross-Murphy, S. B.; Morris, E. R. *Carbohydr. Res.* **1982**, *107*, 17.
(26) Sato, T.; Norisuye, T.; Fujita, H. *Polym. J.* **1984**, *16*, 341.
(27) Yamakawa, H. *Modern Theory of Polymer Solutions*; Harper and Row: New York, 1971.
(28) Norisuye, T.; Yanaki, T.; Fujita, H. *J. Polym. Sci.: Part B: Polym. Phys.* **1980**, 547.
(29) Yanaki, T.; Norisuye, T.; Fujita, H. *Macromolecules* **1980**, 1462.
(30) Norisuye, T.; Xu, X.; Zhang, L.; Nakamura, K. Dilute-Solution Behavior of *Aeromonas* Gum, a Heteropolysaccharide, Conference Proceeding, Euro-Japanese Workshop on Functional Polysaccharides, Kyoto, 2002.
(31) Buckeridge, M. S.; Rocha, D. C.; Reid, J. S. G.; Dietrich, S. M. C. *Physiol. Plant.* **1992**, *86*, 145.
(32) Fanutti, C.; Gidley, M. J.; Reid, J. S. G. *Planta* **1991**, *184*, 137.
(33) York, W. S.; Vanhalbeek, H.; Darvill, A. G.; Albersheim, P. *Carbohydr. Res.* **1990**, *200*, 9.

BM0257659